IOP Publishing Journal of Physics B: Atomic, Molecular and Optical Physics

J. Phys. B: At. Mol. Opt. Phys. **49** (2016) 015601 (8pp) doi:10.1088/0953-4075/49/1/015601

Intensity dependence of the dissociative ionization of DCl in few-cycle laser fields

H Li[1,2], X M Tong[3,4], N Schirmel[5], G Urbasch[5], K J Betsch[1], S Zherebtsov[1], F Süßmann[1], A Kessel[1], S A Trushin[1], G G Paulus[6,7], K-M Weitzel[5] and M F Kling[1,2]

[1] Max-Planck-Institut für Quantenoptik, D-85748 Garching, Germany
[2] Fakultät für Physik, Ludwig-Maximilians-Universität München, D-85748 Garching, Germany
[3] Institute of Materials Science, University of Tsukuba, Ibaraki 305-8573, Japan
[4] Center for Computational Sciences, University of Tsukuba, Ibaraki 305-8577, Japan
[5] Fachbereich Chemie, Philipps-Universität Marburg, D-35032 Marburg, Germany
[6] Institut für Optik und Quantenelektronik, Friedrich-Schiller-Universität Jena, D-07743 Jena, Germany
[7] Helmholtz Institut Jena, D-07743 Jena, Germany

E-mail: tong@ims.tsukuba.ac.jp and matthias.kling@lmu.de

Received 15 July 2015, revised 25 September 2015
Accepted for publication 2 October 2015
Published 24 November 2015

Abstract

We have studied the dissociative ionization of DCl in 4 fs laser fields at 720 nm central wavelength using intensities in the range (1.3–3.1) $\times$ 10^{14} W cm^{-2}. By employing the phase-tagged velocity-map imaging technique, information about the angular distribution of deuterium ions as a function of their kinetic energy and the carrier-envelope phase is obtained. On the basis of the experimental data and semi-classical simulations, three regions are distinguished for the resulting D^+ ions with different kinetic energies. The one with the lowest kinetic energy, around 5–7 eV, is from dissociation involving the X-state of DCl^+, populated through direct ionization with the laser field. The second region, around 7–11 eV, originates from rescattering induced dissociative ionization. Above 2 $\times$ 10^{14} W cm^{-2} D^+ ions with kinetic energies exceeding 15 eV are obtained, which we ascribe to double ionization induced by rescattered electrons.

Keywords: CEP control, attosecond physics, molecular dynamics

(Some figures may appear in colour only in the online journal)

1. Introduction

Short laser pulses of near single-cycle duration open the possibility to control and trace even the fastest molecular processes. In intense laser fields, the ionization of a molecule, the recollisional excitation of a produced ion and its fragmentation can be controlled with the waveform of the electric field [1]. The carrier-envelope phase (CEP) is a commonly used parameter to tailor the electric field $E(t) = E_0\ f(t)\ \cos(\omega t + \psi)$, where E_0 is the field amplitude, $f(t)$ the envelope function, ω the angular carrier frequency, and ψ the CEP. For optical wavelengths the CEP permits to alter the waveform with sub-femtosecond precision.

The effect of sub-cycle modifications of the electric field on molecular processes is of interest both from a fundamental coherent control point of view and in terms of applications of charged-directed chemical reactions [2]. Additionally, such studies also provide fundamental insight into strongly coupled electron-nuclear dynamics, in particular when combined with synchronized attosecond light pulses [3], and into correlated processes such as non-sequential double ionization and how they influence subsequent reaction dynamics [4]. The influence of the CEP on molecular dynamics has primarily been studied for molecular hydrogen and molecular hydrogen ions, both theoretically [5–13] and experimentally [14–25]. The strongly driven electron-nuclear dynamics typically needs to be described by quantum dynamical models beyond the Born–Oppenheimer approximation, which remains challenging for multi-electron molecules. Work on systems beyond molecular hydrogen is therefore desirable, but has so far still been limited. Experimental examples include the sub-cycle control of the ionization and dissociative ionization of

diatomic molecules such as O_2 [26], CO [27–30], DCl [31], and recently also of more complex molecules, including CS_2 [32], N_2O [33], C_{60} [34] and hydrocarbons [4, 35, 36].

The laser intensity is naturally an important parameter in strong-field molecular processes. As an example, recent studies on H_2 [37] and on hydrocarbons [4] have shown that the peak intensity of a few-cycle pulse serves as a control parameter for the electron recollision induced population of excited electronic states of the molecular ion. Another, more extreme example at very high intensities shows that nuclear reactions may be induced by CEP-controlled proton recollisions in molecules [38].

With its large dipole moment, HCl and its isotope DCl are interesting targets for strong-field ionization studies. The potential energy curves and fragmentation channels of the molecular ion have been well documented (see e.g. [39–41]). The interaction with an intense few-cycle pulse leads to tunnel ionization of DCl with the population of the X and A-state of DCl^+ [42]. Both states are stable and dissociation of the molecular ion therefore has to occur through further excitation (e.g. by electron recollision) and/or laser-induced coupling to dissociative states. Akagi *et al* studied the dissociative ionization of HCl in circularly polarized laser fields, omitting electron recollision as an excitation mechanism [42]. Recorded molecular frame photoelectron angular distributions permitted to identify different ionization paths, where the ground X-state is produced by tunnel ionization from the highest-occupied-molecular-orbital (HOMO), and the A-state from the HOMO-1. Dissociation of the molecular ion via bond softening [43] can occur through various photon number pathways via laser-induced coupling of the A state with the dissociative $2^2\Sigma^+$-state [42].

Theoretical studies suggested that due to the influence of the permanent dipole moment, CEP-controlled, linearly polarized few-cycle fields can also induce directionality in the fragment emission in the laser-induced (bond-softening) dissociation of the HCl^+ ion [44]. Further investigations show very large directionality of the D^+ emission from DCl^+ in such laser fields at long wavelengths [45]. An experimental investigation on the dissociative ionization of DCl with few-cycle pulses at 720 nm was conducted at a peak intensity of $1.3 \times 10^{14}\,\mathrm{W\,cm^{-2}}$ [31]. It was observed that the recollision with the electron released in the tunnel ionization of DCl leads to dissociation via excited states of DCl^+. The CEP-dependent directional emission of D^+ and Cl^+ fragments occurs into opposite directions and the optimal CEP for a certain direction is independent of the kinetic energy of the fragments. This behavior was interpreted in terms of an orientation dependence of the tunnel ionization of DCl in the asymmetric few-cycle laser field [31].

Here, we report on extended studies on DCl, where the dissociative ionization in 4 fs laser fields at 720 nm was interrogated for several intensities. In contrast to the studies in [31] the CEP was not stabilized, but instead measured precisely for every single laser shot. This phase-tagging approach [46] provides an improved signal-to-noise ratio in measurements of CEP-dependent molecular processes (see e.g. [35, 36]). The emission of D^+ ions from DCl was monitored with velocity-map imaging (VMI) providing access to their momentum distributions. The angular distribution as a function of CEP provides further insight into the population mechanisms of excited states of the molecular ion.

2. Experimental approach

The phase-tagged VMI setup has been described in detail in [47]. Briefly, a beam of 25 fs pulses centered at 790 nm with a repetition rate up to 1 kHz is obtained from the frontend of the Petawatt-Field Synthesizer at the Max Planck Institute of Quantum Optics [48]. Few-cycle pulses are generated by spectral broadening in a hollow core fiber in combination with pulse compression with chirped mirrors. The resulting pulses have a duration of about 4 fs and are centered at 720 nm. In order to carry out the phase-tagged VMI experiments, the beam is split into two arms, one is sent to a single-shot VMI spectrometer [47] and the other directed to a single-shot phase meter [49], which enables recording the CEP for every single laser shot [46].

The linear polarized 4 fs laser beam is focused into the VMI chamber and intersects with an effusive beam of DCl molecules. The laser intensity is adjusted by a neutral density filter and the peak intensity is estimated from the cutoff energy of rescattered electrons from Xe recorded under identical experimental conditions. The intensity fluctuation of the 4 fs pulses is less than 10%. D^+ ions resulting from the laser–target interaction are projected by the electrostatic lens of the VMI onto a microchannel plate (MCP)/phosphor screen assembly and light flashes from the phosphor screen are recorded with a complementary metal-oxide semiconductor camera at the full repetition rate of the laser. Here the detector lies in the x–y plane, with the laser being polarized along the y-axis. In order to select an ionic species, the MCP voltage is gated by a high-voltage switch at a variable delay with respect to the laser pulse. The gating time window is about 150 ns. The phase-tagging approach permits to record the CEP for each VMI image. The measured CEP has a constant offset to the absolute CEP. In the post-analysis, the recorded data for a CEP range of 2π is binned into 20 images. Finally, the VMI images are inverted to extract a 2D cut around the $p_z = 0$ plane from the 3D momentum distributions [50].

3. Theoretical method

Tunneling ionization is the very first and the most important process for strong field and matter interactions. We describe the process using a single-active-electron model. The single-electron Hamiltonian is approximated

$$H = T + V_{\mathrm{Cl}}(r_1) + V_{\mathrm{D}}(r_2) + V_{\mathrm{C}}(r), \qquad (1)$$

with T the kinetic operator, $V_{\mathrm{Cl}/D}(r_{1/2})$ the potential of the active electron due to the interaction with Cl/D ions and $r_{1/2}$ the distance of the electron to the Cl/D nucleus. The term $V_{\mathrm{C}}(r) = \mathrm{Erf}(\alpha r)/r$, a positive potential, is introduced to

compensate the spurious Coulomb interaction when the DCl is in the united atom limit with r being the distance from the electron to the geometrical center. V_{Cl} is calculated from density functional theory with self-interaction correction [51]. We chose $\alpha = 0.48$ since the ionization potentials of HOMO and HOMO-1 obtained from the model potential are in good agreement with the reported ones [52]. With the diatomic molecular model potential we calculate the ionization probabilities of DCl in a 5 fs Gaussian pulse (static field) by solving the time-dependent Schrödinger equation in spheroidal coordinates [53, 54]. The Cl atom is assumed to be placed in the positive direction of the molecular axis. The orientation dependent ionization probability mimics the π orbital electron density with minimum along the molecular axis and maximum in the perpendicular directions. Due to the unbalanced electron nuclear core interaction, the ionization probability reaches a maximum at about $\theta = 60°$.

We assume that the orientation dependent tunneling ionization rates are expressed as

$$R(\theta, E) = R_1(\theta)R_2(E), \tag{2}$$

with $R_1(\theta)$ the orientation dependent part, which is proportional to the ionization probability calculated above and $R_2(E)$ the field strength dependent part, which is calculated by the modified atomic tunneling ionization model [55]. Note that in reality, the orientation dependent ionization rates also depend on the peak intensity. Thus the total ionization probability of DCl in an oscillating field can be expressed as

$$P(\theta, \phi) = \int_{-\infty}^{+\infty} R_1(\theta)R_2(E(t))\mathrm{d}t|_{E(t)>0} + \int_{-\infty}^{+\infty} R_1(\pi - \theta)R_2(E(t))\mathrm{d}t|_{E(t)<0}. \tag{3}$$

Here ϕ is the CEP. The laser intensity and CEP information is included in $E(t)$, which can be expressed as $E(t) = E_0 f(t) \cos(\omega t + \psi)$. From a symmetry point of view, the dissociation $DCl^+ \rightarrow D + Cl^+$ occurs through a σ orbital, or the HOMO-1 orbital. From earlier results obtained for DCl [31], we can infer that the dissociation is not sensitive to the CEP, thus we calculate the dissociation yield on the up/down half-sphere as

$$Y_{up}(\phi) = \int_0^{\pi/2} P(\theta, \phi)\cos^2(\theta)\sin\theta\mathrm{d}\theta,$$
$$Y_{down}(\phi) = \int_{\pi/2}^{\pi} P(\theta, \phi)\cos^2(\theta)\sin\theta\mathrm{d}\theta. \tag{4}$$

Here we assume the dissociation rate is proportional to $\cos^2\theta$ since the major dissociation channel correlates with the HOMO-1, a σ state. The asymmetry parameter is defined as

$$A(\phi) = \frac{Y_{up}(\phi) - Y_{down}(\phi)}{Y_{up}(\phi) + Y_{down}(\phi)}. \tag{5}$$

Similarly, the rescattering induced double ionization probability is estimated as

$$P^{++}(\theta, \phi) = \int_{-\infty}^{+\infty} R_1(\theta)R_2(E(t))P_{res}(E(t)) \times \mathrm{d}t|_{E(t)>0} + \int_{-\infty}^{+\infty} R_1(\pi - \theta)R_2(E(t)) \times P_{res}(E(t))\mathrm{d}t|_{E(t)<0} \tag{6}$$

Here P_{res} is the rescattering electron impact ionization probability, which includes two simulations. We first calculate the returning electron energy and impact parameter from a semi-classical simulation and then calculate the impact ionization probability by using an empirical ionization cross section as in [56]. With $P^{++}(\theta, \phi)$, the asymmetry parameters due to rescattering induced double ionization can be obtained.

4. Results and discussion

4.1. Momentum distributions and kinetic energy spectra of D^+ ions

Momentum images and the corresponding angle integrated energy spectra of D^+ fragment ions from the dissociative ionization of DCl at several intensities are shown in figure 1. These images are cuts through the 3D momentum distributions around $p_z = 0$ obtained by inversion. The background signal below 8 a.u. (0.2 eV) is mainly from leakage of the neighboring H^+ signal due to its close time of flight, therefore it is subtracted from the D^+ images.

For the lowest intensity we explored, the momentum map is similar to what was observed in a previous study [31]. The angular distribution of D^+ ions peaks at about 60° with respect to the laser polarization direction. This angle is in good agreement with expectations for the tunnel ionization from the degenerate HOMOs of DCl as further detailed below. A few sharp rings are visible in the D^+ momentum distribution, which indicate contributions from several excited states of DCl^+. As the laser intensity increases, ions with higher momenta are obtained. This becomes more obvious in the energy spectra shown in figure 1(e). These spectra are obtained from integration of the D^+ momentum distributions within an angle range of ±20° with respect to the y-axis. For the highest intensity used in our study, peaks in a high kinetic energy region (above 15 eV) can be distinguished, which lie at around 16.8 eV and 19.3 eV. In the presence of the strong laser field, the required energy for the population of highly excited dissociative states of DCl^+ can be acquired via electron recollision. The maximum recollision energy can be classically estimated as 3.17 U_p, where U_p is the ponderomotive potential, defined as $U_p = I/(4\omega^2)$ (a.u.) for the laser intensity I. Within the studied intensity range we obtain maximum recollision energies between 20 eV (1.3×10^{14} W cm^{-2}) and 47 eV (3.1×10^{14} W cm^{-2}). These

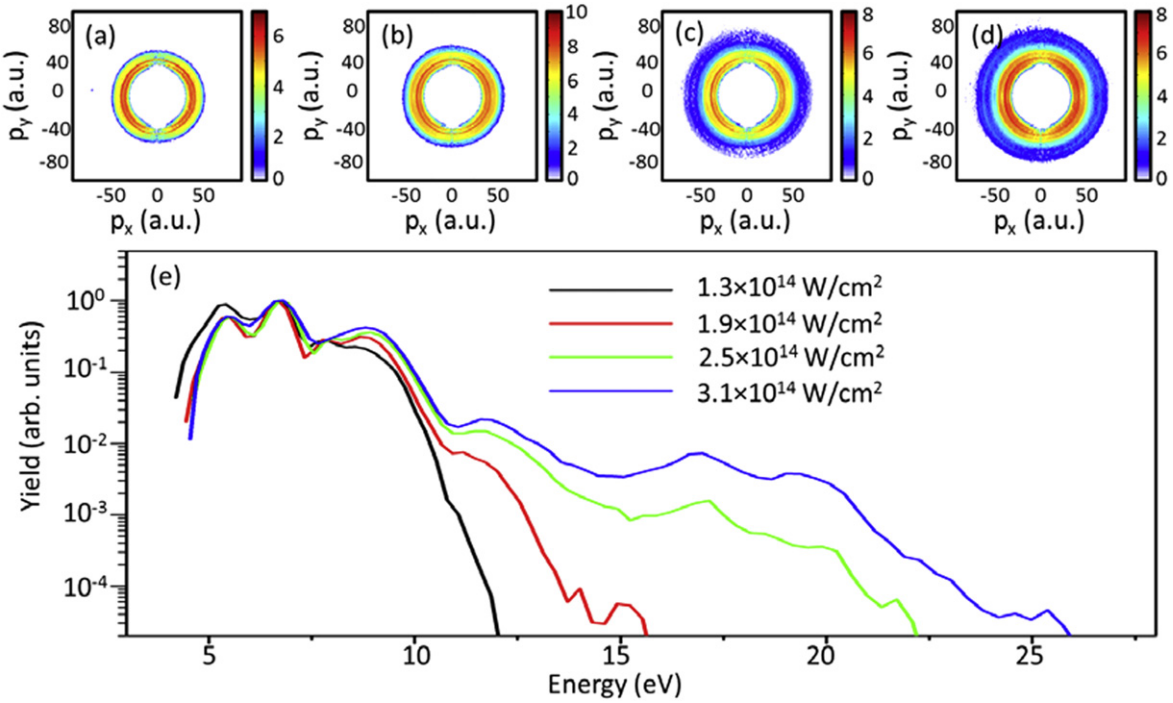

Figure 1. (a)–(d) CEP-averaged momentum distributions of D^+ ions from the dissociative ionization of DCl with 4 fs pulses at 720 nm at intensities of (1.3, 1.9, 2.5 and 3.1) $\times$ 10^{14} W cm^{-2}, respectively. Note that the intensity uncertainty is around $\pm$20%. (e) The corresponding energy spectra for D^+ for the above intensities, respectively. The spectra are normalized to the peak at 6.8 eV, the strongest peak observed.

energies are sufficient to populate the excited states of DCl^+ and the intensity dependence of the maximum recollision energy can explain the increasing peak height of higher energy contributions in the D^+ spectra in figure 1(e). By inspection of the data shown in figure 1 we can conclude the following: (i) dissociative ionization involving DCl^+ is the main channel for the production of D^+ ions between momenta of 33 and 54 a.u., and (ii) D^+ ions with higher momenta above 60 a.u. (kinetic energy above 15 eV), marginally observed for the highest intensities, might arise from Coulomb explosion of DCl^{2+}.

4.2. Directional emission of fragment ions

The CEP-dependence of the directional emission of D^+ fragments from the dissociative ionization of DCl is investigated by analyzing the energy-dependent asymmetry parameter, which is defined as

$$A(W, \phi) = \frac{N_+(W, \phi) - N_-(W, \phi)}{N_+(W, \phi) + N_-(W, \phi)}, \qquad (7)$$

with W being the ion kinetic energy, and $N_+(W,\phi)$ and $N_-(W, \phi)$ being the yields in positive and negative p_y direction, respectively. The resulting asymmetry maps are shown in figures 2(a)–(c) for intensities of (1.3, 2.5 and 3.1) $\times$ 10^{14} W cm^{-2}, respectively. Experimental data are obtained for CEPs from 0 to 2π. For better visibility, the data from 2π to 4π are reproduced from the measured data.

Significant asymmetries within the energy ranges of the detected species are observed. They vary as a function of CEP, demonstrating the strong-field control of the processes leading to the dissociative ionization of DCl. These processes involve the ionization of DCl, electron recollisional excitation and potentially also laser coupling between DCl^+ states during the dissociation. In contrast to the observation in a previous study [31] (which employed phase stabilization instead of phase tagging and therefore had limited signal-to-noise ratio), the oscillation of the asymmetry parameter with CEP for the D^+ ions is found to be kinetic energy dependent. Two major regions can be distinguished for D^+ at about 1.3 $\times$ 10^{14} W cm^{-2} (figure 2(a)), one at 5–7 eV and the other at 7–11 eV, with a characteristic phase offset in the asymmetry oscillation between them. The phase shift between the above two regions can be clearly distinguished in the plot of energy-integrated asymmetry parameters in figure 2(g). The first region (5–7 eV) can be assigned to dissociation involving the X-state of DCl^+. The population of the X-state occurs through direct ionization with the laser field, and the asymmetry consequently peaks around CEP = 0 at 1.3 $\times$ 10^{14} W cm^{-2}. The second region, found at higher energies (7–11 eV) and exhibiting higher asymmetry values, yields a phase shift in the asymmetry oscillation of about 0.2π with respect to the low energy region (5–7 eV). Ions in this region might originate from dissociation involving the A-state of DCl^+, populated by rescattering induced ionization. The angular distribution of the asymmetry amplitude in the range of 7–11 eV resembles the orientation-dependent ionization probability of the HOMOs of DCl, which is shown in figure 3 and generally agrees with earlier observations [31].

With the intensity increasing, as shown in figures 2(a)–(c), the amplitude of the asymmetry oscillation within the energy region of 5–7 eV becomes smaller, and the maximum

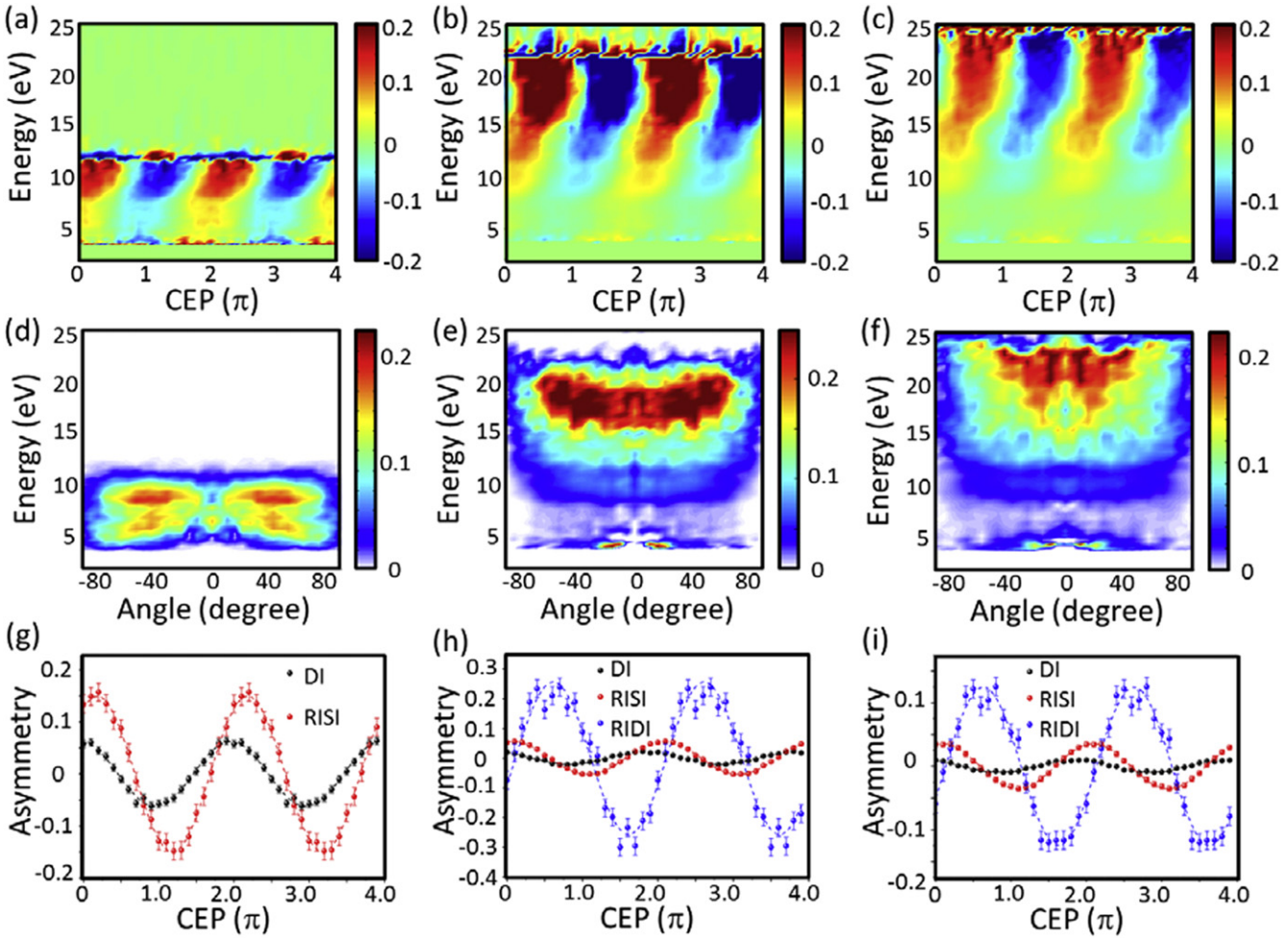

Figure 2. (a)–(c) Asymmetry maps for D^+ ions as a function of CEP and kinetic energy at intensities of (1.3, 2.5 and 3.1) $\times$ 10^{14} W cm^{-2}, respectively. For better visibility, the data within 2π to 4π is reproduced from those from 0 to 2π. The sudden change close to the cutoff region is due to the selection of an extra factor which is added to the denominator when calculating the experimental asymmetry parameter (as is shown in equation (7)). Distribution of the absolute value of the asymmetry amplitude (d)–(f) as a function of angle and kinetic energy for the intensities mentioned above. Here the angle is defined with respect to the laser polarization direction. These plots are symmetrized around 0°. (g)–(i) Energy-integrated asymmetry parameters as a function of CEP for the direct ionization (DI), the rescattering induced single ionization (RISI), and the rescattering induced double ionization (RIDI) regions, at the above intensities, respectively. The dashed curves are the fitting results to a cosine function.

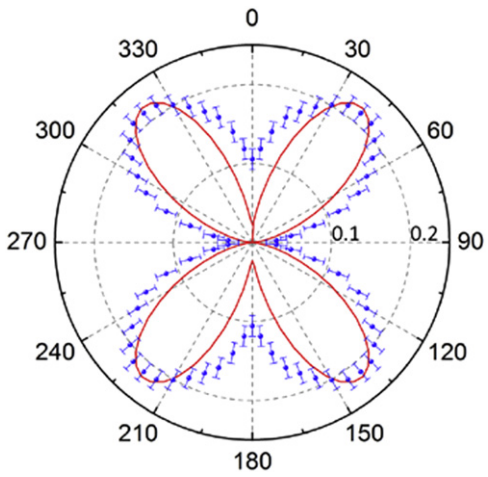

Figure 3. Polar plot of the energy-integrated (7–11 eV) asymmetry derived from figure 2(d) and the calculated ionization probability (solid line) from the HOMOs of DCl.

is shifted toward negative CEPs. Our simulation results represent a similar trend for the asymmetry amplitude as a function of laser intensity, with some discrepancy in the absolute values, as shown in table 1. For sufficiently intense laser fields, in which the DCl^+ ions can be dissociated completely at any CEP, the asymmetry amplitude would go to zero. Table 1 shows this trend. The relative asymmetry phase shift for this region can be attributed to a change in return energy of the released electron as a function of intensity.

The third region with even higher kinetic energy (>12 eV) is observed for intensities of 2.5 and 3.1 $\times$ 10^{14} W cm^{-2}. In this region, the asymmetry exhibit high amplitude (up to about 30%) with its maximum at around 0.63π. Such a phase shift with respect to direct ionization is indicative of a double ionization process induced by rescattered electrons, see e.g. [33, 57, 58]. The separation of the dissociation into three regions is further supported by the plots of energy-integrated asymmetry as a function of CEP, as

Table 1. Comparison of asymmetry amplitudes for the direct ionization channel (5–7 eV) at different laser intensities.

Intensities ($\times 10^{14}$ W cm^{-2})	1.3	2.5	3.1
Asym. amp. (experiment)	(6.2 ± 0.3)%	(2.1 ± 0.1)%	(0.9 ± 0.05)%
Asym. amp. (theory)	2.3%	0.8%	1%

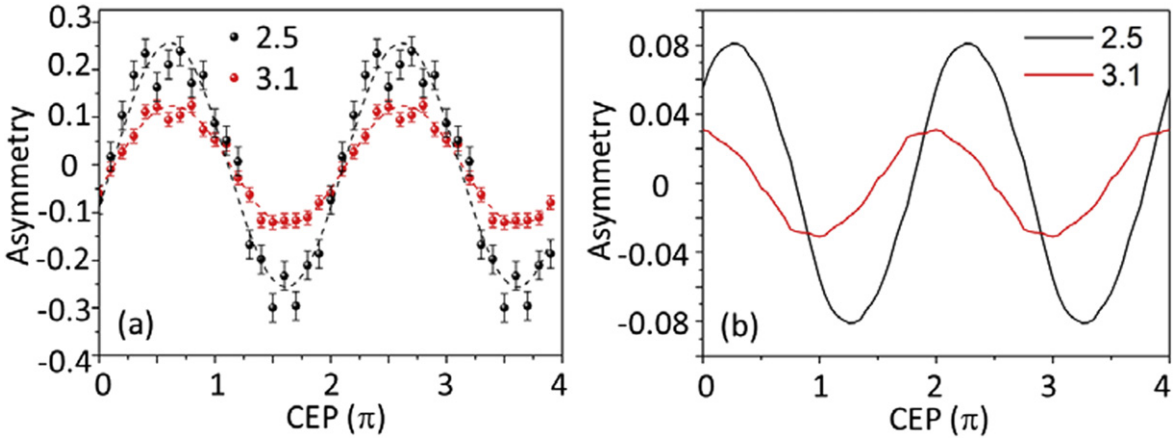

Figure 4. Asymmetry parameters obtained from experiment (a) and semi-classical calculation (b) for rescattering induced double ionization at intensities of 2.5 and 3.1 $\times$ 10^{14} W cm^{-2}, respectively. The dashed lines in (a) are sinusoidal fits to the data.

shown in figures 2(g)–(i). There are clear phase shifts between the three regions mentioned above.

The rescattering electron impact ionization probability in equation (6) is about 7 orders smaller than the dissociative single ionization at 1.3 $\times$ 10^{14} W cm^{-2} and 5 orders smaller at 1.9 $\times$ 10^{14} W cm^{-2} in our simulation. This can be understood as that although at 1.9 $\times$ 10^{14} W cm^{-2} the maximum returning electron energy is about 30 eV, higher than the ionization potential (23.8 eV) of DCl^+, the rescattering electron yield is very small since it is created by tunneling ionization at a half cycle before the laser field reaches its maximum. In contrast, for electrons tunneling out at the peak laser field and successively accelerated by the laser field, the return energy is lower than the ionization potential. Thus, this channel for intensities below 2 $\times$ 10^{14} W cm^{-2} is negligible. However, for higher intensities, double ionization is only about 2 to 3 orders smaller than the dissociative single ionization. Therefore the contribution to the asymmetry parameter is significant. The fragmentation after double ionization results in a high kinetic energy of the resulting ions through Coulomb repulsion. The rescattering electron energy is sensitive to the CEP and the asymmetry parameters will therefore peak at a different phase. Figure 4 shows the comparison between measured and simulated asymmetry parameters for rescattering induced double ionization at intensities of 2.5 and 3.1 $\times$ 10^{14} W cm^{-2}. Experimental data show a decreasing in asymmetry amplitude for higher laser intensity, with almost no phase offset. The theoretical results can reproduce the tendency in the change of asymmetry amplitude, with somewhat discrepancy on the phase offset. Here we use a two-step simulation. Firstly, the average returning time and returning energy are calculated by a semi-classic trajectory, and then we assume that the ions are ionized at the returning time with the returning energy. There is a sharp returning time and energy for a relative low intensity. But for high intensity, the returning electrons exhibit a broad energy distribution and we do not have reliable cross section information to model the process accurately. The amount of theoretical work will increase dramatically if we trace all the trajectories. On the other hand, the asymmetry parameters obtained from experiment are higher than the theoretical values, as is shown in both table 1 and figure 4. The way of processing the experimental data might play a big role here. According to equation (7), by removing larger background signal, the resulting asymmetry parameter will show a higher value. Besides this, the tendency in the asymmetry amplitude is well reproduced by the calculations and qualitatively explains the change of the asymmetry amplitude for high and low kinetic energy regions for different laser intensities.

5. Conclusions

We have investigated the dissociative ionization of DCl in intense few-cycle laser fields within the intensity range of (1.3–3.1) $\times$ 10^{14} W cm^{-2}. Significant CEP-dependent asymmetries in the directionality of the ejection of D^+ ions are observed. By investigating the asymmetry parameter as well as its angular distribution, we find the following mechanisms. (i) Dissociation occurring after single ionization through tunneling dominates the directional ion emission at 5–7 eV. As laser intensity increases, the amplitude of the asymmetry parameter in this region becomes smaller, which can be explained by the decreasing of sensitivity to the CEP and the molecular orientation for higher laser intensities. (ii) Excitation of the molecular ion via electron rescattering generates D^+ ions with higher kinetic energy (7–11 eV). (iii) For intensities above 2 $\times$ 10^{14} W cm^{-2}, D^+ ions above 15 eV are

observed and originate from rescattering induced double ionization. With a simple semi-classical model, we can qualitatively explain the characteristics of asymmetry in this region. Theory results predict a smaller amplitude for the asymmetry oscillation for higher laser intensity, which agrees with the experimental results. However, the phase shift observed is not well-reproduced by the simulation. The agreement at 2.5×10^{14} W cm^{-2} is better on both asymmetry amplitude and phase, which shows that our theoretical model works well for intermediate laser intensities. For high intensity, the returning energy has a broad distribution. With reliable cross section information and tracing all the trajectories, it will be possible to obtain a better theory prediction for what we observed here.

Acknowledgments

We are grateful to F Krausz for his support. We acknowledge experimental support by Nora G Kling with the phase meter. We are grateful for support by the Max Planck Society and the DFG via the Cluster of Excellence: Munich Center for Advanced Photonics (MAP). XMT was supported by a Grand-in Aid for Scientific Research (C24540421) from the Japan Society for the Promotion of Science and HA-PACS (Highly Accelerated Parallel Advanced system for Computational Sciences) Project for advanced interdisciplinary computational sciences by exascale computing technology.

References

[1] Kling M F, von den Hoff P, Znakovskaya I and de Vivie-Riedle R 2013 (Sub-)femtosecond control of molecular reactions via tailoring the electric field of light *Phys. Chem. Chem. Phys.* **15** 9448

[2] Weinkauf R, Schanen P, Yang D, Soukara S and Schlag E W 1995 Elementary processes in peptides: electron mobility and dissociation in peptide cations in the gas phase *J. Phys. Chem.* **99** 11255–65

[3] Lepine F, Sansone G and Vrakking M J J 2013 Molecular applications of attosecond laser pulses *Chem. Phys. Lett.* **578** 1–14

[4] Xie X *et al* 2012 Attosecond-recollision-controlled selective fragmentation of polyatomic molecules *Phys. Rev. Lett.* **109** 243001

[5] Bandrauk A D, Chelkowski S and Nguyen H S 2004 Attosecond localization of electrons in molecules *Int. J. Quantum Chem.* **100** 834–44

[6] Roudnev V, Esry B D and Ben-Itzhak I 2004 Controlling HD^+ and H_2^+ dissociation with the carrier-envelope phase difference of an intense ultrashort laser pulse *Phys. Rev. Lett.* **93** 163601

[7] Tong X M and Lin C D 2007 Carrier-envelope phase dependence of nonsequential double ionization of H_2 by few-cycle laser pulses *J. Phys. B: At. Mol. Opt. Phys.* **40** 641–9

[8] Gräfe S and Ivanov M Y 2007 Effective fields in laser-driven electron recollision and charge localization *Phys. Rev. Lett.* **99** 163603

[9] Geppert D, von den Hoff P and de Vivie-Riedle R 2008 Electron dynamics in molecules: combination of nuclear quantum dynamics and electronic structure theory *J. Phys. B: At. Mol. Opt. Phys.* **41** 074006

[10] He F, Becker A and Thumm U 2009 Strong-field modulated diffraction effects in the correlated electron-nuclear motion in dissociating H_2^+ *Phys. Rev. Lett.* **101** 213002

[11] Kelkensberg F, Sansone G, Ivanov M Y and Vrakking M 2011 A semi-classical model of attosecond electron localization in dissociative ionization of hydrogen *Phys. Chem. Chem. Phys.* **13** 8647–52

[12] Anis F and Esry B D 2012 Enhancing the intense field control of molecular fragmentation *Phys. Rev. Lett.* **109** 133001

[13] He F 2012 Control of electron localization in the dissociation of H_2^+ using orthogonally polarized two-color sequential laser pulses *Phys. Rev.* A **86** 063415

[14] Kling M F *et al* 2006 Control of electron localization in molecular dissociation *Science* **312** 246

[15] Kling M F, Siedschlag C, Znakovskaya I, Verhoef A J, Zherebtsov S, Krausz F, Lezius M and Vrakking M J J 2008 Strong-field control of electron localization during molecular dissociation *Mol. Phys.* **106** 455–65

[16] Kremer M *et al* 2009 Electron localization in molecular fragmentation of H_2 by carrier-envelope phase stabilized laser pulses *Phys. Rev. Lett.* **103** 213003

[17] Fischer B, Kremer M, Pfeifer T, Feuerstein B, Sharma V, Thumm U, Schröter C-D, Moshammer R and Ullrich J 2010 Steering the electron in H_2^+ by nuclear wave packet dynamics *Phys. Rev. Lett.* **105** 223001

[18] Sansone G *et al* 2010 Electron localization following attosecond molecular photoionization *Nature* **465** 763–6

[19] Singh K P *et al* 2010 Control of electron localization in deuterium molecular ions using an attosecond pulse train and a many-cycle infrared pulse *Phys. Rev. Lett.* **104** 023001

[20] Kelkensberg F *et al* 2011 Attosecond control in photoionization of hydrogen molecules *Phys. Rev. Lett.* **107** 043002

[21] Znakovskaya I *et al* 2012 Sub-cycle controlled charge-directed reactivity with few-cycle mid-infrared pulses *Phys. Rev. Lett.* **108** 063002

[22] Kling N G *et al* 2013 Carrier-envelope phase control over pathway interference in strong-field dissociation of H_2^+ *Phys. Rev. Lett.* **111** 163004

[23] Xu H, Maclean J-P, Laban D E, Wallace W C, Kielpinski D, Sang R T and Litvinyuk I V 2013 Carrier-envelope-phase-dependent dissociation of hydrogen *New J. Phys.* **15** 023034

[24] Rathje T, Sayler A M, Zeng S, Wustelt P, Figger H, Esry B D and Paulus G G 2013 Coherent control at its most fundamental: carrier-envelope-phase-dependent electron localization in photodissociation of a H_2^+ molecular ion beam target *Phys. Rev. Lett.* **111** 093002

[25] Xu H, Xu T-Y, He F, Kielpinski D, Sang R T and Litvinyuk I V 2014 Effect of nuclear mass on carrier-envelope-phase-controlled electron localization in dissociating molecules *Phys. Rev.* A **89** 041403

[26] Siu W *et al* 2011 Attosecond control of dissociative ionization of O_2 molecules *Phys. Rev.* A **84** 063412

[27] von den Hoff P, Znakovskaya I, Kling M F and de Vivie-Riedle R 2009 Attosecond control of the dissociative ionization via electron localization: a comparison between D_2 and CO *Chem. Phys.* **366** 139–47

[28] Znakovskaya I, von den Hoff P, Zherebtsov S, Wirth A, Herrwerth O, Vrakking M J J, de Vivie-Riedle R and Kling M F 2009 Attosecond control of electron dynamics in carbon monoxide *Phys. Rev. Lett.* **103** 103002

[29] Liu Y, Liu X, Deng Y, Wu C, Jiang H and Gong Q 2011 Selective steering of molecular multiple dissociative channels with strong few-cycle laser pulses *Phys. Rev. Lett.* **106** 073004

[30] Betsch K J *et al* 2012 Controlled directional ion emission from several fragmentation channels of CO driven by a few-cycle laser field *Phys. Rev.* A **86** 063403
[31] Znakovskaya I, von den Hoff P, Schirmel N, Urbasch G, Zherebtsov S, Bergues B, de Vivie-Riedle R, Weitzel K M and Kling M F 2011 Waveform control of orientation-dependent ionization of DCl in few-cycle laser fields *Phys. Chem. Chem. Phys.* **13** 8653–8
[32] Mathur D, Dota K, Dharmadhikari A K and Dharmadhikari J A 2013 Carrier-envelope-phase effects in ultrafast strong-field ionization dynamics of multielectron systems: Xe and CS_2 *Phys. Rev. Lett.* **110** 083602
[33] Kübel M *et al* 2014 Strong-field control of the dissociative ionization of N_2O with near single-cycle pulses *New J. Phys.* **16** 065017
[34] Li H *et al* 2015 Coherent electronic wave packet motion in C_{60} controlled by the waveform and polarization of few-cycle laser fields *Phys. Rev. Lett.* **114** 123004
[35] Alnaser A S *et al* 2014 Subfemtosecond steering of hydrocarbon deprotonation through superposition of vibrational modes *Nat. Commun.* **5** 3800
[36] Miura S *et al* 2014 Carrier-envelope-phase dependence of asymmetric CD bond breaking in C_2D_2 in an intense few-cycle laser field *Chem. Phys. Lett.* **595–6** 61–6
[37] Li H *et al* 2014 Intensity dependence of the attosecond control of the dissociative ionization of D_2 *J. Phys. B: At. Mol. Opt. Phys.* **47** 124020
[38] Lötstedt E and Midorikawa K 2014 Nuclear reaction induced by carrier-envelope-phase controlled proton recollision in a laser-driven molecule *Phys. Rev. Lett.* **112** 093001
[39] Breunig H G, Lauer A and Weitzel K M 2006 *J. Phys. Chem.* A **110** 6395–8
[40] Korolkov M V and Weitzel K M 2006 On the competition between predissociation and direct dissociation in deuterium chloride ions (DCI+) *J. Chem. Theory Comput.* **2** 1492–8
[41] Pradhan A D, Kirby K P and Dalgarno A 1991 Theoretical study of HCl^+: potential curves, radiative lifetimes, and photodissociation cross sections *J. Chem. Phys.* **95** 9009
[42] Akagi H, Otobe T, Staudte A, Shiner A, Turner F, Dörner R, Villeneuve D M and Corkum P B 2009 Laser tunnel ionization from multiple orbitals in HCl *Science* **325** 1364–7
[43] Bucksbaum P H, Zavriyev A, Muller H G and Schumacher D W 1990 Softening of the H_2^+ molecular bond in intense laser fields *Phys. Rev. Lett.* **64** 1883–6
[44] Abou-Rachid H, Nguyen-Dang T T and Atabek O 1999 Dynamical quenching of laser-induced dissociations of heteronuclear diatomic molecules in intense infrared fields *J. Chem. Phys.* **110** 4737–49
[45] Korolkov M V and Weitzel K M 2007 Laser pulse control of photofragmentation in DCI+: the effect of carrier envelope phase *Chem. Phys.* **338** 277–84
[46] Rathje T, Johnson N G, Möller M, Süßmann F, Adolph D, Kübel M, Kienberger R, Kling M F, Paulus G G and Sayler A M 2012 Review of attosecond resolved measurement and control via carrier-envelope phase tagging with above-threshold ionization *J. Phys. B: At. Mol. Opt. Phys.* **45** 074003
[47] Süßmann F *et al* 2011 Single-shot velocity-map imaging of attosecond light-field control at kilohertz rate *Rev. Sci. Instrum.* **82** 093109
[48] Ahmad I *et al* 2009 Frontend light source for short-pulse pumped OPCPA system *Appl. Phys.* B **97** 529–36
[49] Wittmann T, Horvath B, Helml W, Schätzel M G, Gu X, Cavalieri A L, Paulus G G and Kienberger R 2009 Single-shot carrier-envelope phase measurement of few-cycle laser pulses *Nat. Phys.* **5** 357–62
[50] Vrakking M J J 2001 An iterative procedure for the inversion of two-dimensional ion/photoelectron imaging experiments *Rev. Sci. Instrum.* **72** 4084–213
[51] Tong X-M and Chu S-I 1997 Density-functional theory with optimized effective potential and self-interaction correction for ground states and autoionizing resonances *Phys. Rev.* A **55** 3406–16
[52] Natalis P, Pennetreau P, Longton L and Collin J E 1982 Ionization energy values for the vibronic transitions from HCl $X^1\Sigma^+$ ($v'' = 0$) to HCl^+ ionic states $X^2\Pi$ ($v' = 0$–13) and $A^2\Sigma+$ ($v' = 0$–12), determined by photoelectron spectroscopy *J. Electron Spectrosc. Relat. Phenom.* **26** 173
[53] Chu X and Chu S-I 2001 Self-interaction-free time-dependent density-functional theory for molecular processes in strong fields: High-order harmonic generation of H_2 in intense laser fields *Phys. Rev.* A **63** 023411
[54] Jin Y-J, Tong X-M and Toshima N 2012 Anomalous alignment dependence of the third-order harmonic of H_2^+ ions in intense laser fields *Phys. Rev.* A **86** 053418
[55] Tong X M and Lin C D 2005 Empirical formula for static field ionization rates of atoms and molecules by lasers in the barrier-suppression regime *J. Phys. B: At. Mol. Opt. Phys.* **38** 2593–600
[56] Tong X M, Zhao Z X and Lin C D 2003 Correlation dynamics between electrons and ions in the fragmentation of D_2 molecules by short laser pulses *Phys. Rev.* A **68** 043412
[57] Bergues B *et al* 2012 Attosecond tracing of correlated electron-emission in non-sequential double ionization *Nat. Commun.* **3** 813
[58] Kübel M *et al* 2013 Non-sequential double ionization of N_2 in a near single-cycle laser pulse *Phys. Rev.* A **88** 023418